CIENCIA 4(4), 323-334, 1996
Maracaibo, Venezuela

Theoretical study of the metallo-porphyrin adsorption on a hematite cluster

Leonardo J. Rodríguez and Juan J. Chirinos*

Laboratorio de Química Teórica y Computacional (LQTC). Departamento de Química
Facultad Experimental de Ciencias. La Universidad del Zulia, Apartado. 526
Maracaibo 4001-A, Venezuela

Recibido 09-08-96 Aceptado: 23-11-96

Abstract

The adsorption geometries of unsubstituted vanadyl porphyrin on a hematite cluster were studied by means of MINDO/SR method. A survey of diatomic parameters for MINDO was carried out in order to reproduce the experimental values of bond length, dissociation energy and spectroscopic multiplicity for all diatomic pairs formed by Fe, V, C, N, H and O. Models for hematite and unsubstituted vanadyl porphyrin were constructed. Six adsorption geometries were calculated and their adsorption energy curves were plotted. Four adsorption geometries result to be totally repulsive, whereas the two others shown a minimum value in adsorption energy curve. Nevertheless, only one of these minimum have positive adsorption energy. Thus, only one of the studied geometries represent an effective adsorption site. This geometry involves the interaction between an iron atom of the hematite and the π bond of the pyrrole ring in the metallo porphyrin. Due to the softening of some bonds and the changes in the atomic charge of some atoms, we conclude that the adsorption of the metallo porphyrin on a hematite cluster produce the activation of the meso position of the porphyrin for early hydrogenation.

Key words: HDM; hematite; MINDO/SR; vanadyl porphyrin.

Estudio teórico de la adsorción de metalo-porfirinas sobre un agregado de hematita

Resumen

Las geometrías de adsorción de la vanadil porfirina no substituida sobre un agregado de hematita fueron estudiadas por medio del método MINDO/SR. Se realizó un reconocimiento de los parámetros diatómicos del MINDO para reproducir los valores experimentales de distancia de enlace, energía de disociación y multiplicidad espectroscópica para todas las parejas diatómicas formadas por Fe, V, C, N, H y O. Se construyeron modelos para la hematita y la vanadil porfirina no substituida. Fueron calculadas seis geometrías de adsorción y sus curvas de energía de adsorción fueron graficadas. Cuatro geometrías de adsorción resultaron ser totalmente repulsivas, mientras que las otras dos mostraron un valor mínimo en la curva de energía de adsorción. Sin embargo, sólo una de estas geometrías representan un sitio de adsorción efectivo. Esta geometría envuelve la interacción entre un átomo de hierro de la

* To whom correspondence will be addressed. E-mail: leon@solidos.ciens.luz.ve.

hematita y el enlace π del anillo pirrólico en la metalo porfirina. Debido al debilitamiento de algunos enlaces y a los cambios en la carga de algunos átomos, concluimos que la adsorción de la metalo porfirina sobre un agregado de hematita produce la activación de la posición meso de la hematita para las primeras hidrogenaciones.

Palabras claves: HDM; hematita; MINDO/SR; vanadil porfirina.

Introduction

The heterogeneous catalysis of hydrodemetallization (HDM) is the most employed processes for metals elimination in heavy crude oils (1). The majority of metals in crudes are associated with asphaltenes and part of these forms organometallic complexes like metalloporphyrin (MP). These MPs are structures with very high stability and represent a serious problem for the conventional refining processes. In the HDM processes, the irreversible deposition of a certain amount of metal on the active sites of catalysts is unavoidable. Thus, the deposited metal acts as catalyst poisons and it requires catalyst regeneration in order to restore their activity.

Solutions of synthetic MP as model molecules are treated with the catalysts under very drastic temperature and pressure conditions in HDM laboratory studies. Only, in few cases, the heavy crude is directly analyzed due to the complexity of the reaction. The vanadium and nickel are the metals most usually found in the MPs of heavy crude oils. The high levels of metals, asphaltenes, sulfur, nitrogen and oxygen, plus the high viscosity of the heavy crude oils, require upgrading of these crudes to meet internationally allowed levels.

The most common HDM catalysts are various metal transition oxides with Ni and Co as promoters. The use of mixtures of metal oxides is also very useful, where the control of metal concentrations ratio is important. On the other hand, the use of natural clay as HDM catalyst has shown to be an efficient and economic process (2). The study of the active phases of HDM catalyst by Mössbauer absorption spectroscopy (3) shows the presence of small hematite particles coming from the calcining of small geothite particles. In view of the fact that more than 50% of the iron present in the clay is found forming part of the hematite, the study of the MP-hematite interaction was undertaken in the present work.

An important detail in the initial phases of HDM process is the adsorption geometry of the MP on the surface of the catalyst. The adsorption geometry is a crucial factor in the catalytic process, and the efficiency of the reaction will depend of the geometric interaction between the adsorbate and the adsorbent. For this reason, we have focus our attention over this point. On the other hand, exist many controversies in the literature about the mechanism of MP demetallation. One of the most accepted idea about the HDM mechanism explain that the MP undergo structural changes that involve, loss of aromatic character by hydrogenation prior to cleavage of the ring and deposition of the metal (4). Thus, for the study of the HDM catalysis the knowing of the electronic and bonding properties of the reactants and product are required.

As far as we know, this work is the first theoretical work concerning the interaction between a MP complex and a hematite cluster. Recently, Rodriguez *et. al.* (5) studied the H_2 adsorption over Fe_2O_3 clusters. One of the principal objectives of this work is to analyze the variations of the electronic properties as a consequence of the adsorption. In particular, we want to know if the MP is activated in the adsorption process. The term activation here means the softening of the any bond in the MP structure.

In the present work, the MINDO/SR method was applied to investigate the adsorption geometries of the unsubstituted metalloporphyrin (UMP) on a hematite cluster. The variations of the electronic properties were analyzed in order to explain the adsorption process.

Calculation Procedure

The calculations were carried out employing a semi-empirical self-consistent-field method referred as MINDO/SR (6), which is a modified version of MINDO/3 (7) that include the transition metals in the calculation. The computer program is based on QCPE-290 algorithm, described by Rinaldi (8), with automatic geometry optimization using analytically calculated gradients. The version used in this work is able to read the Hartree-Fock matrix of the fragments from previously optimized calculations. The latter is useful in the accelerating electronic convergence (9).

The Slater-Condon parameters, the Slater exponent orbitals and core parameters for Fe, V, N, C, H y O, used in this work, have been taken from the literature (5,6, 10-15). The bonding parameters for the corresponding diatomic pairs were adjusted after a search of the different electronic configurations of the diatomic molecules. In particular, the parametrization of the inter metallic pair Fe-V, was performed due to the lack of data for this molecule. This parametrization process will be explained in the next section.

Results and discussion

Diatomic Molecules

Before setting out to examine the MP adsorption results over a hematite cluster, an analysis of the search of bonding parameters for the diatomic molecules is presented. All the parameters used in this work were obtained following a rigorous method to guarantee the following properties: (a) the diatomic molecule must be in its ground state. (b) the interatomic distance was taken from the experimental bond length, (c) the calculated gradient is always lower than 10^{-4} and (d) our calculations reproduce, in very good agreement, the experimental enthalpy of formation.

The diatomic parameters for the elements C, H, N and O are reported (7). For pairs formed by iron and these elements the diatomic parameters are also reported (15). However, for pairs involving the vanadium atom there are few parameters. Recently, a MINDO/SR parametrization was carried out for homonuclear diatomic molecules of the first transition metal series (13). However, for intermetallic molecule there is not information in the literature. A curious case is the FeV molecule. The molecule FeV is a thirteen electrons system, and the most energetic electron is located in a non-bonding molecular orbital; thus, the ion FeV^+ is more stable than the FeV molecule. For this reason, the equilibrium bond length and dissociation energy data for this diatomic molecule are incomplete in the literature. To overcome this difficulty we make an estimation of the dissociation energy from the thermodynamic data for FeV diatomic species (16) and using the following Born Haber cycle:

$$FeV^+ \longrightarrow Fe + V^+ \qquad D^\circ_{(FeV+)}$$

$$FeV \longrightarrow FeV^+ \qquad IP_{(FeV)}$$

$$V^+ \longrightarrow V \qquad IP_{(V)}$$

$$FeV \longrightarrow Fe + V \qquad D^\circ_{(FeV)}$$

Thus, the dissociation energy is: $D^\circ_{(FeV)} = D^\circ_{(FeV+)} + IP_{(FeV)} - IP_{(V)}$ .Where D° is the dissociation energy and IP is the ionization potential. On the other hand, the interatomic distances for FeV was taken as the sum of the atomic radius of Fe and V.

The final bonding parameters from this analysis are given in Table 1. Some parame-

ters of this Table were taken from the literature and other parameters were obtained of this work; but in all cases, the parameters were tested here. The results obtained in the present work show that it is possible to obtain more stable states than found in previous calculations (20).

Hematite Cluster

Hematite has a corundum structure (21,22), which is rombohedral with space group D^6_{3d}(R3c). It consists of an approximately hexagonal closed-packed (HCP) array of oxygen atom in which the metal atoms occupy two-thirds of the octahedral holes.

Table 1
Diatomic Parameters

Molecule	α	β	Mult.[a]	$r_{eq.}$(Å)[a]	$D^o_{(exp.)}$	$D^o_{(calc.)}$
H-H	1.48945[b]	0.24477[b]	1	0.74116	-104.0	-103.2
C-C	0.84860[c]	0.35751[c]	1	1.2425	-142.0	-142.1
N-N	0.45958[c]	0.72900[c]	1	1.0977	-225.07	-225.17
O-O	0.82604[c]	0.64466[c]	3	1.20741	-118.0	-118.08
Fe-Fe	0.44317[d]	0.47027[d]	5	2.02	-24.2	-24.0
Fe-H	1.25700[d]	0.41000[d]	6	1.50	-82.0	-82.0
Fe-C	1.38000[e]	1.06000[e]	3	1.8 (3)	-56.07	-60.6
Fe-N	0.59000[f]	0.60700[f]	2	1.84	-209.03	-209.4
Fe-O	1.75703[d]	1.06944[d]	5	1.626	-90.3	-90.3
Fe-V	10.3525[c]	7.58449[c]	2[c]	1.895[c]	-44.3[c]	-44.5
V-H	1.63540[c]	0.52406[c]	3	1.59	-49.126	-49.66
V-C	0.68991[c]	0.71034[c]	2[g]	1.577[g]	-156.14[g]	-156.1
V-N	0.75845[c]	0.67225[c]	3	1.5666	-114.1	-114.33
V-O	0.59887[c]	0.81677[c]	4[h]	1.589[h]	-148.8[h]	-148.53
O-H	0.47890[b]	0.41776[b]	2	0.9706	-101.0	-94.9
O-C	0.15531[c]	1.19549[c]	1	1.12832	-225.8	-255.44
O-N	0.46782[c]	0.86354[c]	2	1.1508	-150.71	-155.72
N-H	1.32469[c]	0.53283[c]	3	1.045	-75 (4)	-75.3
N-C	0.69788[c]	0.46957[c]	2	1.17198	-184.1	-183.93
C-H	0.73430[c]	0.31900[c]	2	1.1202	-80.0	-80.8

[a] Reference 17; [b] Reference 7; [c] This work; [d] Reference 5; [e] Reference 6; [f] Reference 15; [g] Reference 18; [h] Reference 19.

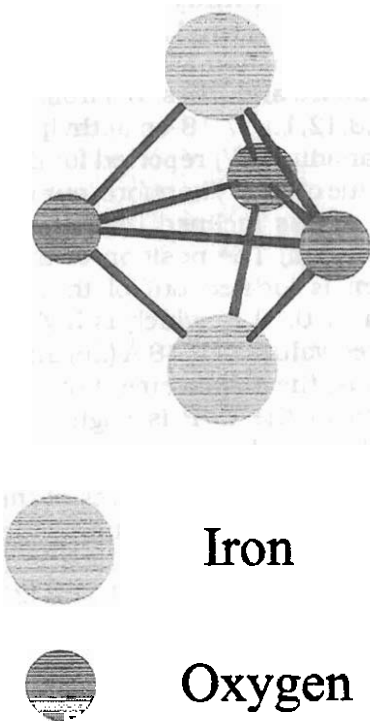

Figure 1. A pluto drawing of the hematite structure.

In order to represent the hematite surface in a simple way, a cluster of five atoms (Fe_2O_3) was employed and is shown in Figure 1. The main reasons for this selection are:

a) A complete deoxygenated surface is assumed because, during the HDM reaction, continual hydrogen flow over the catalyst causes removal of the superficial oxygen atoms, leaving them available for a direct interaction with the adsorbate.

b) A small-size cluster is suitable for calculations of chemisorption of UMP that contains 38 atoms. It is worthwhile to mention that the use of the UMP and the small hematite cluster is imperative in this work due to the limited capacity of our computer.

c) The fact that the total charge on our model is zero gives more realistic energy levels, because highly charged clusters produce, as in other calculations (23), occupied levels with positive energy values.

At this point, it is worthwhile to mention that our model is quite different from the usual hematite bulk models selected in the literature, where a distorted octahedral structure is represented by a central iron atom and six oxygen atoms with a total charge of -9 to simulate the oxidation state of +3 for the iron atom.

In order to analyze the hematite properties, the Mulliken Bond Orders (MBO) and the electronic populations will be used and compared with the FeO diatomic molecule. The MBOs indicated that the strongest bond in hematite correspond to Fe-O (MBO = 0.55). However, the Fe-O bond in hematite is considerably weaker than in the diatomic molecule (MBO = 1.28). This is due to a smaller interatomic overlap arising from a longer Fe-O equilibrium interatomic distance in hematite (2.116 Å) than in the FeO molecule (1.626 Å), and to a greater coordination number in the oxygen as well as in the iron atoms. On the other hand, the O-O interaction is very small (MBO = 0.005) and repulsive, which is in agreement with previous results (24).

The calculated electronic populations for the iron atoms was 0.403 a.u. ($s^{0.596}$, $p^{0.958}$, $d^{6.043}$) and for the oxygen atoms was -0.269 a.u. ($s^{1.681}$, $p^{4.588}$). This reveals that the Fe-O bond is relatively covalent with some ionic character. An *ab-initio* study over hematite reports a charge transfer of 0.29 a.u. from O to Fe (25).

All calculations were carried out by considering the most stable spin multiplicity. In this case, the optimal multiplicity for the hematite cluster is 9, which is associated to a spin magnetic moment of 4.0 μB. This optimal multiplicity value corresponds to 8 unpaired electrons; however, the experimental value of 4.7 μB (25) seems to indicate that the number of the unpaired electrons must be 9.

The unsubstituted Vanadyl-porphyrin (UVP)

The optimized structure obtained for the UVP is shown in Figure 2. In this Figure the numeration used in the calculation for some selected atoms was included to facilitate the reading of the tables. In this structure, the vanadium atom (V1) is five coordinated to four nitrogen atoms in the plane of the porphyrin and to one oxygen atom (O2) located perpendicular to the porphyrin plane. Thus, the vanadium is the central atom of the pyramidal square base structure. There are two interesting features of this pyramid that it is worth to be mentioned: (i) the V=O vector is tilted 0.2° with respect to the normal of the porphyrin plane and the difference is too small to be visible in the Figure. This inclination of the oxygen atom was first reported by Petersen (26) to present a value of 2° by studying a single crystal of vanadyl deoxophyllo-erythroetioporphyrin-1,2-dichloroethane from x-ray diffraction (XRD). On the other hand, Molinaro and Ibers (27) from XRD for the 2,3,7,8,12,13,17,18-octaethylporphyrinatooxovanadium(IV) reported for the same angle a value of 1.2°. Therefore, our modeled structure is less inclined than the experimental ones. (ii) The position of the vanadium atom is located out of the plane of porphyrin by 0.59 Å, which is higher than the reported values of 0.48 Å (26) and 0.543 Å (27). Thus, the displacement of the vanadium atom in the UVP is slightly smaller than a substituted ones.

Other geometrical features of the UVP structure are the following: The average V-N bond distances is 2.56 Å, which is higher than the reported value of 2.102 Å (26) and

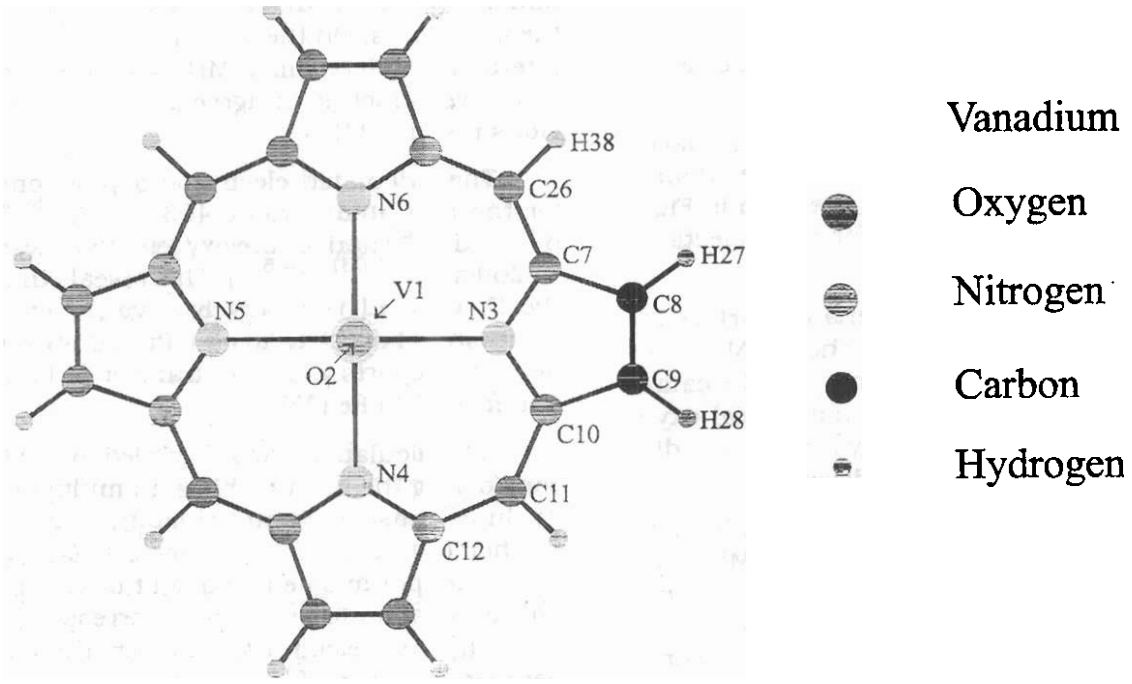

Figure 2. A pluto drawing of the UVP structure. The atomic numeration used in the calculation is shown for selected atoms.

1.96 Å (27). As a consequence of this result we obtained a very low value for the MBO for this bond (0.303). This last result suggests that there is a relaxation effect when the porphyrin are not substituted with respect to substituted ones. The optimized V-O bond length is 1.659 Å, and this value is in agreement with the values reported (26-27).

A comparison of our optimized structure with octaethylporphyrin (28) free base shows that the insertion of VO for H has a minimal effect on the geometry of the porphyrin core. Of course, the porphyrin core is far less planar in the vanadyl complex. In general, we found that the UVP structure does not present a major change with respect to the results obtained from XRD for a variety of MP. For this reason, the use of the UVP for our calculations is feasible for modeling the UVP-hematite interaction.

Metalloporphyrin adsorption

In this study, the term adsorption energy represents the difference between the total energy of the MP-hematite system and the sum of the total energies of the hematite and the MP molecule separated at infinity. A stable adsorption state of MP molecule would have a negative value of adsorption energy.

A simulation of the MP adsorption over an hematite cluster requires a large number of calculations due to the fact that the approach of the MP may occur in different way and may involve various sites of adsorption. However, considering only the chemical situation with most probabilities of interaction, the number of geometries may be reduced to six. The six adsorption geometries studied in this work are show in Figure 3. In this figure the hydrogen atoms have been omitted for clarity.

The geometry called G1 implies the interaction between an iron atom of the hematite and the oxygen atom (O2) of the UVP, where the plane of the UVP is parallel to the ecuatorial plane of the hematite. In this case, the iron atom acts as an acceptor group and the oxygen atom as a donor group. The other interaction possibility for the oxygen in the UVP will be with other oxygen of the hematite; but this interaction was not considered due to its obvious repulsive character. The geometries G2 and G3 consist of the interaction between the vanadium atom (V1) of the UVP with an oxygen atom and an iron atom of the hematite, respectively. The plane of the UVP with respect to the ecuatorial plane of the hematite is perpendicular for G2 and parallel for G3. However, in these two geometries the approach between the UVP and hematite occurs for the opposite face to the V=O group; but, in G1 the approach occurs for the face with the V=O group. The geometries G4 and G5 are related due to the interaction between an external π bond (C8 y C9) of the pyrrole ring of the UVP and one oxygen atom and one iron atom of the hematite, respectively. In G4, the line connecting the two iron atom of the hematite is in the same plane of the UVP, and in G5 the ecuatorial plane of the hematite is perpendicular to the UVP plane. Finally, the G6 geometry implies the interaction between an iron atom of the hematite with the center of the one pyrrole ring of the UVP. In this geometry the UVP plane is parallel to the ecuatorial plane of the hematite and the interaction occurs in the opposite plane to the V=O group.

In Figure 4, we summarized the six absorption energy curves against interaction distance. It is important to point out that we optimized the multiplicity in all calculations, however, in Figure 4 only the optimal multiplicities are depicted. For the G1 geometry a minimal energy was found about 2.0 Å; however, the absorption energy was lightly positive, indicating that this geometry is an unstable absorption site. For the G2 and G3 cases, we find that the curves are totally repulsive, i.e., their curves do not present any minimum over all the range of interaction distances studied. Particularly,

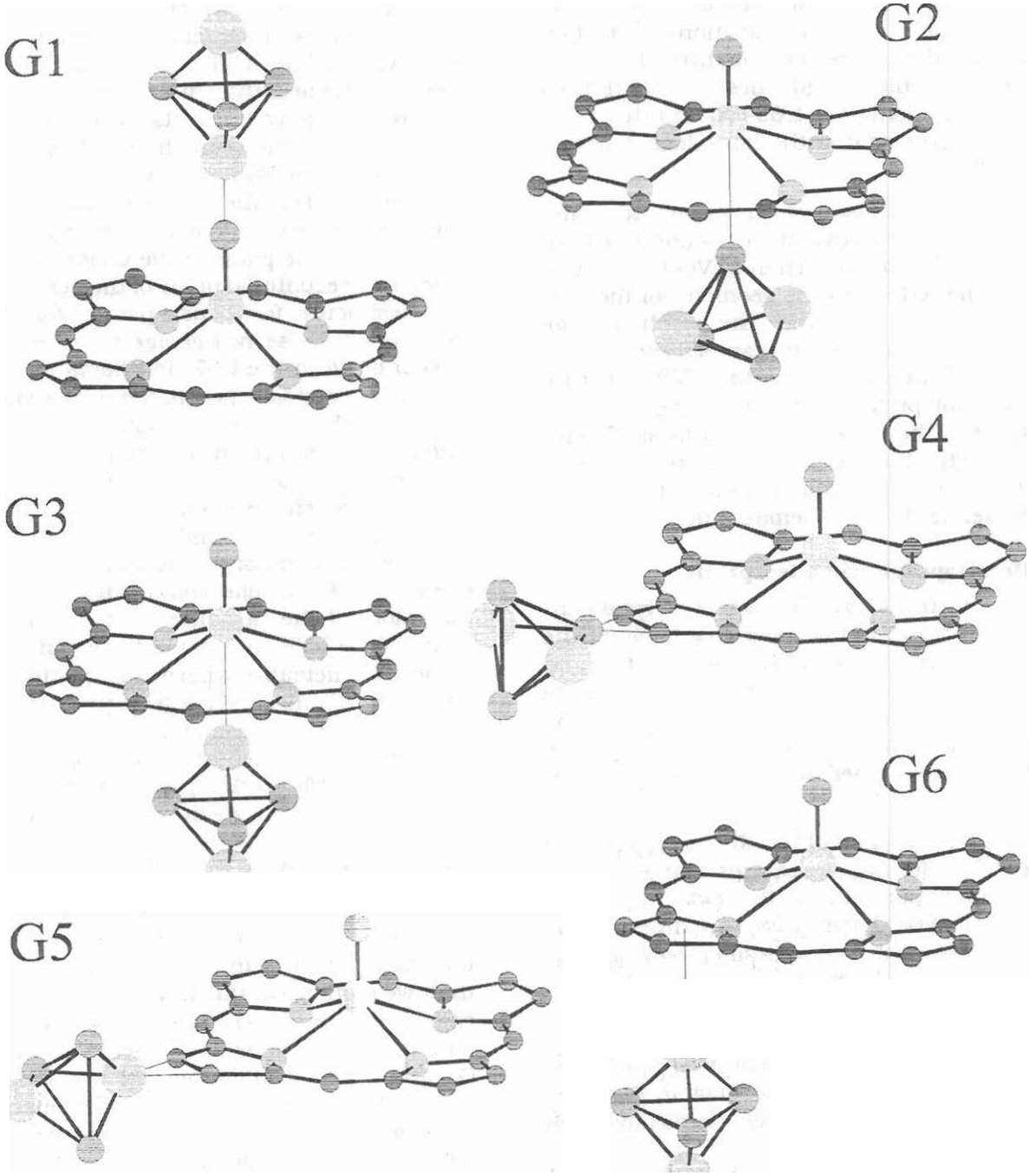

Figure 3. A pluto drawing of the six adsorption geometries. The hydrogen atoms have been omitted for clarity.

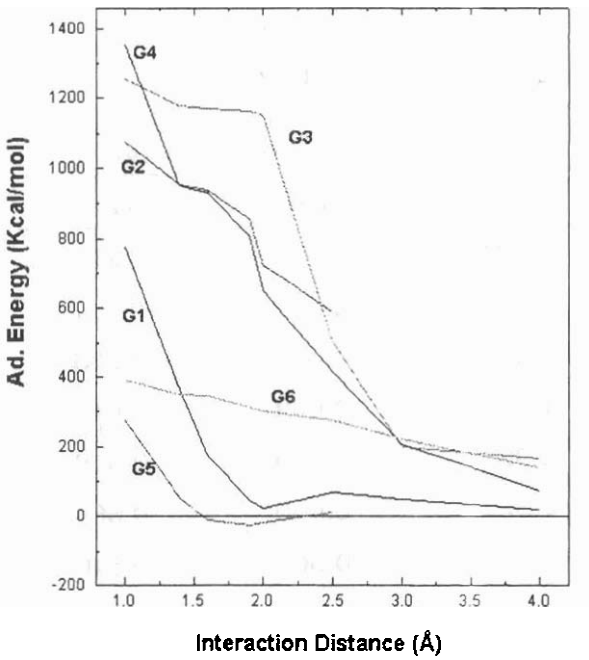

Figure 4. Adsorption energy curves for the six

the G3 geometry presents a very high adsorption energy at interaction distances lower than 2 Å, indicating that this intermetallic interaction is not energetically favored. For the G2 geometry, the calculations were carried out using a range of interaction distances, starting at 1 Å until 2.5 Å. Beyond this distance no convergence was obtained for the electronic energy. The results obtained for G2 and G3 reveal the non-participation of the vanadium atom in the adsorption process.

For the G4 geometry, the Figure 4 shows a curve of adsorption energy totally repulsive. This is due to the nucleophilic character of the two interacting parts. From the studied geometries, the G4 presented the highest adsorption energy at 1 Å. For the G5 geometry, we obtain a minimum in the absorption energy curve. In this case, the interaction is between an iron atom with atomic charge of 0.40 u.e. with the double bond carbon-carbon with a mean atomic charge of -0.06. Thus, this geometry is very favored by the electrostatic attraction. Additionally, the approach of the UVP to the iron atom does not show steric problems. For the G5, we obtain that the absorption energy is -25.11 Kcal/mol at 1.9 Å. Finally, the adsorption energy curve for the G6 geometry results repulsive with a lowest slope of the studied geometries.

In Table 2 are collected some MBO and diatomic energy for the isolated fragments (at infinity distance) and for the geometry G5 with multiplicity 8. As consequence of the adsorption, the following remarks must be mentioned: (a) the Fe-O bond in the hematite becomes weak after the adsorption due to the participation of the iron atom in new interactions with carbon and hydrogen atoms of the UVP. Obviously, when the iron atom increases its coordination number, their bonds softening to compensate its bonding capacity; (b) the V=O and V-N bonds remain practically unaltered, because the interaction is located far from the vanadium atom; (c) the C8-C9 bond, which initially formed a double bond becomes weak in the G5 geometry by its interaction with the iron atom of the hematite. Due to the fact that interaction in G5 geometry is with two atoms, the rotation here is constrained and these calculations were not considered; (d) the bonds C8-H27 and C9-H28 become weak too for the reasons mentioned above; (e) two new strong bonds are formed between the iron atom of the hematite with the carbons C8 and C9 of the UVP, and (f) two new weak bonds are formed between the iron atom of the hematite with the hydrogen H27 y H28.

Therefore, the adsorption geometry G5 significantly changes the bonding and electronic properties of the interacting parts. It is worthwhile to explain the change of the atomic density in the carbon atom (C11) located in the meso position of the porphyrin. In the isolated UVP this atom had an atomic charge of 0.004 u.e.; whereas, in the G5 geometry its atomic charge is -0.177 u.e.. This represents an important increase in its negative charge and this atom becomes a reactive site for hydrogenation

Table 2
Mulliken bond orders and diatomic energies of hematite, UVP and G5

Molecule	bond	MBO		diatomic energy	
		isolated	G5	isolated	G5
hematite	Fe-O	0.573	0.194	-0.373	-0.277
	O-O	0.012	-0.003	-0.114	+0.017
	Fe-Fe	0.467	0.433	-0.021	-0.033
UVP	V1-O2	1.037	1.036	-0.642	-0.643
	V1-N3	0.314	0.325	-0.049	-0.058
	N3-C7	1.359	1.387	-0.640	-0.665
	C7-C8	1.269	1.287	-0.503	-0.510
	C8-C9	1.933	1.649	-0.798	-0.607
	C9-C10	1.258	1.226	-0.497	-0.502
	C10-C11	1.473	1.476	-0.600	-0.609
	C11-C12	1.419	1.385	-0.567	-0.555
	C8-H27	1.220	1.034	-0.432	-0.322
	C9-H28	1.212	1.027	-0.431	-0.320
	C11-H29	1.201	1.238	-0.425	-0.429
	C26-H38	1.203	1.204	-0.426	-0.426
	Fe-C8	0.000	1.011	0.000	-0.612
	Fe-C9	0.000	1.015	0.000	-0.616
	Fe-H27	0.000	0.441	0.000	-0.059
	Fe-H28	0.000	0.443	0.000	-0.060

when the UVP is adsorbed over hematite in G5 geometry.

Thus, we can conclude that the UVP is activated in G5 geometry for two reasons. First, the softening of the some bonds in the UVP introduce important electronic changes that make the UVP more reactive. Second, the increase of the negative atomic charge on the carbon atom in meso position facilitate its hydrogenation.

Conclusions

An adequate parametrization of the MINDO/SR method produced excellent results for the studied diatomic molecules.

The interaction between the iron atom of the hematite with an oxygen atom or with a π ring is unfavorable, as indicated by the results for the geometries G1 and G6.

The vanadium atom of the UVP does not participate in the adsorption process, as indicated by the results for the geometries G2 and G3. Thus, the removal of the metal from the UVP in the HDM is non-selective.

The geometry G4 that implies the interaction between two nucleophilic fragments is totally repulsive.

The G5 geometry was the only stable adsorption site. This case implies that the iron atom interacts with a π bond of the pyrrole ring of the UVP. Here, at 1.9 Å of interaction distance the adsorption energy was -25.0 Kcal/mol.

The softening of the some bonds and the increase of the negative charge in the carbon atom in meso position of the UVP is an evidence of the metallo porphyrin activation.

Acknowledgment

The authors would like to express their gratitude to Consejo Nacional de Investigaciones Científicas y Tecnológicas CONICIT for the center assistance # F-139. We are grateful to Alfonso Chirinos and Humberto Soscun for helpful discussions.

References

1. GATES B. ***Catalytic Chemistry***. John Wiley & Sons, Inc. New York (USA), 1992.
2. ROSA-BRUSSÍN M. ***Catal Rev Sci Eng*** 37(1): 1, 1995.
3. GONZÁLEZ-JIMÉNEZ H., IRALDI C.R., JAIMES E., ROSA-BRUSSIN M. ***Hyp Int*** 28: 927, 1986.
4. WARE R.A., WEI J. ***J of Catal*** 93: 122, 1985.
5. RODRÍGUEZ L.J., RUETTE F., ROSA-BRUSSIN M. ***J Mol Catal*** 62: 199, 1990.
6. BLYHOLDER G., HEAD J., RUETTE F. ***Theor Chim Acta*** 60: 429, 1982.
7. BINGHAM R.C., DEWAR M.J.S., LO D.H. ***J Am Chem Soc*** 97: 1285, 1975.
8. RINALDI D. ***Comput Chem*** 1: 109, 1976.
9. HEAD J., BLYHOLDER G., RUETTE F. ***J of Comp Phys*** 45: 255, 1982.
10. CLEMENTI E., RAIMONDI D.L. ***J Chem Phys*** 38: 2686, 1963.
11. DE BROUCKÈRE G. ***Theoret Chim Acta*** 19: 310, 1970.
12. ANDERSON W.P., EDWARDS W.D., ZERNER M.C. ***Inor Chem*** 25: 2728, 1986.
13. RODRÍGUEZ L.J., RUETTE F. ***J Mol Struct (Theochem)*** 287: 179, 1993.
14. KARLSSON G. ZERNER M. ***Int J Quant Chem*** VII: 35, 1973.
15. RINCÓN L., RUETTE F., HERNÁNDEZ A. ***J Mol Struct (Theochem)*** 254: 395, 1992.
16. HETTICH R.L., FREISER B.S. ***J Am Chem Soc*** 107: 6222, 1985.
17. ROSEN B. ***Spectroscopic Data to Diatomic Molecules***. Pergamon Press, Oxford, New York (USA), 1978.
18. MATTAR S.M. ***J Phys Chem*** 97: 3171, 1993.
19. COPPENS P., SMOES S., DROWART J. ***J Chem Soc Faraday Trans*** 63: 2140, 1967.
20. RODRÍGUEZ L.J., RUETTE F., CASTRO G.R., LUDEÑA E.V., HERNÁNDEZ E.V. ***Theor Chim Acta*** 77: 39, 1990.
21. BLAKE R.L., HESSEVICK R.E., FINGER L.W. ***Am Mineralogist*** 51: 123, 1966.
22. FASISKA E.J. ***Corrosion Sci*** 7: 833, 1967.
23. SHERMAN D.M. ***Phys Chem Min*** 12: 161, 1985.
24. KELIRES P.C., DAS T.P. ***Hyp Int*** 34: 285, 1987.

25. CATTI M., VALERIO M., DOVESI M. ***Phys Rev B*** 51: 7441, 1995.

26. PETTERSEN R.C. ***Acta Cryst*** B25: 2527, 1969.

27. MOLINARO F.S., IBERS J.A. ***Inorg Chem*** 15: 2278, 1976.

28. LAUHER J.W., IBERS J.A. ***J Am Chem Soc*** 95: 5140, 1973.